Full scale investigation of GCL damage mechanisms in small earth dam retrofit applications under earthquake loading

Sawada, Yutaka
Nakazawa, Hiroshi
Take, W. Andy
Kawabata, Toshinori

(Citation)
Geotextiles and Geomembranes,47(4):502-513

(Issue Date)
2019-11-13

(Resource Type)
journal article

(Version)
Accepted Manuscript

Full scale investigation of GCL damage mechanisms in small earth dam retrofit applications under earthquake loading

Yutaka Sawada[a], Hiroshi Nakazawa[b], W. Andy Take[c] and Toshinori Kawabata[d]

[a] Assistant Professor, Graduate School of Agricultural Science, Kobe University, 1-1 Rokkodai, Nada-ku, Kobe, Hyogo, 657-8501, Japan, E-mail: sawa@harbor.kobe-u.ac.jp

[b] Senior Researcher, National Research Institute for Earth Science and Disaster Resilience, 3-1, Tennodai, Tsukuba, Ibaraki, 305-0006, Japan, E-mail: nakazawa@bosai.go.jp

[c] Professor, GeoEngineering Centre at Queen's - RMC, Queen's University, 58 University Ave, Kingston, Ontario, Canada K7L 3N6, E-mail: andy.take@queensu.ca

[d] Professor, Graduate School of Agricultural Science, Kobe University, 1-1 Rokkodai, Nada-ku, Kobe, Hyogo, 657-8501, Japan, E-mail: kawabata@kobe-u.ac.jp

The corresponding author

Yutaka Sawada, Phone: +81 78 803 5902, E-mail: sawa@harbor.kobe-u.ac.jp

ABSTRACT

This paper reports results of full scale testing to further explore potential GCL damage mechanisms in earth dam retrofit applications in seismically active areas; in particular, to a) investigate whether shear displacements could reduce the magnitude of GCL panel overlap during earthquake shaking; b) explore the influence of gravel particles on GCL thickness at localised point of contact; and c) observe the consequences of an accidental exposure of an uncovered GCL to short duration rainfall in terms of moisture content and effects during subsequent compaction. The results of these experiments indicate that even under severe shaking no movements were detected at the GCL panel overlap. Whereas gravel particles were observed to locally reduce the thickness of the GCL to 2.2 mm, no plowing of the particle into the GCL occurred due to a lack of shear displacement at the interface, resulting in no localized internal erosion through the barrier. Furthermore, hydration of GCL panels during construction due to surface wetting was observed to result in a state of hydration less than its post-construction state. These results indicate that although each of the three GCL damage mechanisms cannot be ruled out to ever be relevant in practice, the performance of the GCL retrofitted earth dam tested was satisfactory under even severe Level 2 earthquake shaking, and suggests that the retrofitting of small earth dams with GCLs is a promising strategy to improve their static and seismic resistance.

KEY WORDS: Earth dam; Full-scale shaking table test; Geosynthetic clay liner

1 INTRODUCTION

Japan has over 200,000 small earth dams within use in the agricultural industry, the majority of which were constructed more than 150 years ago without modern compaction control and knowledge of soil mechanics. These legacy infrastructure assets are typically 3-10 m high and pose a risk of static failure (e.g. piping, overtopping, shear failure during extreme rainfall) as well as exhibiting poor earthquake resistance (Ministry of Agriculture, Forestry and Fisheries, 2018). In response to this concern, a program of earth dam retrofitting has been undertaken to improve the static and seismic resistance of these structures. The conventional method to repair small earth dams is to install a sloping core layer at the upstream side of the dam using cohesive soils to form a low permeability zone. However, in recent years, sources of high-quality cohesive soil near dam sites has been exhausted. Therefore, geosynthetic clay liners (GCLs), have also been used to repair deteriorated small earth dams (e.g. Aoyama, 2011). An example of such a retrofit is shown in Figure 1. This construction photograph has been included as it is useful to introduce three important considerations regarding the use of GCLs in earth dam applications within seismically active zones.

The first consideration relates to the possible influence of GCL panel overlaps on the seismic stability of the upstream face. GCLs are shipped to site on rolls of a prescribed width and length. As in landfill barrier system applications for side slopes, GCLs are typically placed with the roll direction aligned

with the downslope direction of the slope. Adjacent GCL panels are not typically bonded to each other, but rather, are overlapped a prescribed distance with powdered supplemental bentonite often added to the lapped joint to ensure adequate hydraulic performance. In addition to these lateral GCL panel overlaps, it is also possible for lapped joints to be introduced into the system in the downslope direction to minimize product wastage (i.e. it is unlikely that roll length is an integer multiple of the required product placement length), or operational considerations during construction such as the efficiency of compaction. As shown in Figure 1, the introduction of a lapped joint in the downslope direction could enable the timely placement and compaction of cover soil using a bottom-up construction method. Such a scenario avoids the undesirable situation where large surface areas of GCL are left exposed to rainfall causing initial hydration of the bentonite core to occur under low normal stress conditions. However, it is unclear whether a lapped joint in the downslope direction inadvertently introduces a point of weakness into the barrier system. If the GCL experiences tension during earthquake shaking, it is unclear whether a lapped joint (especially one containing hydrated supplemental bentonite gel) could experience sufficient shear displacements to reduce the overlap sufficiently to compromise the effectiveness of the hydraulic barrier.

A second consideration for the use of GCLs in earth dams relates to the prevention of internal erosion through the bentonite core of the GCL. Despite the carefully prepared foundation layer at the moment of GCL panel installation illustrated in Figure 1, it is possible that gravel particles contained within the

typically non-select well graded earth dam materials exist at the surface of the compacted foundation soil or at the base of the covering soil layer. Work on the use of GCLs in landfill liner applications by Dickinson and Brachman (2010) have shown that localised thinning of a GCL's bentonite core can occur at points of localised contact with gravel particles, lowering the total head required to initiate internal erosion of the bentonite core. This is of significance as hydraulic heads within earth dam applications will be generally higher than landfill liner applications due to the presence of the water reservoir in the former, and leachate collection systems in the latter. Furthermore, in a base landfill liner application, a gravel particle indenting a GCL is generally expected to fill the void it created. In the seismic loading of an earth dam, any downslope relative displacement of the indenting gravel particle and the GCL during earthquake shaking has the potential to plow an elongated void within the GCL that exceeds the dimensions of the particle. Further work is therefore required to investigate localised GCL thinning during construction of earth dams and the potential for subsequent damage during seismic events.

A third consideration relates to the protection of the GCL during the installation process; in particular, to define the boundary conditions controlling the timing and rate of initial hydration of the GCL. Work from the use of GCLs in landfill liner applications has shown that initial hydration of the bentonite core under low normal stress conditions leads to higher moisture contents, bulk void ratios, and higher hydraulic conductivities of GCLs (e.g. Petrov et al., 1997; Lake and Rowe, 2000; Beddoe et al., 2011). In contrast, GCLs hydrating through the uptake of moisture from the foundation soil do so at a rate

related to the moisture content of the foundation soil (e.g. Rayhani et al., 2011; Rowe et al., 2011; Siemens et al., 2012; Anderson et al., 2012; Sarabian and Rayhani, 2013). This slower rate of hydration ensures sufficient time prior to full hydration for the placement and compaction of cover soil to occur and the GCL subjected to beneficial normal stress prior to reaching its final moisture content. Unconfined hydration of the GCL during exposure to rainfall is therefore undesirable, with construction inspectors often requiring tarps anchored with sand bags (Figure 1) to provide temporary protection from rainfall. However, no guidance exists to construction inspectors in Japan regarding whether the accidental exposure of a GCL to short duration rainfall could result in only a modest increase in moisture content and no adverse effects during subsequent compaction.

The performance of GCLs in earth dam retrofit applications has recently been investigated at full scale in shaking table tests on 3 m high water retaining dam models (Sawada et al., 2016; Oda et al., 2016; Nakazawa et al., 2017; Sawada et al., 2018). Of particular note, Sawada et al. (2018) report the seismic performance of an earth dam retrofitted with continuous GCL (i.e. no lapped joints in the downslope direction) under seismic motion up to 470 Gal (Figure 2a). This dam was observed to experience settlement and longitudinal cracking due to preferential downslope displacement towards the reservoir under this severe loading scenario. Despite this shear displacement, no leakage was observed through the GCL, illustrating that earth dams with continuous GCL layers in the downslope direction with carefully prepared foundation and cover soils to remove gravel particles are likely to have sufficient

seismic resistance to permit downstream evacuation.

The objective of this work is to conduct additional full scale testing to further explore potential GCL damage mechanisms in earth dam retrofit applications in seismically active areas; in particular, to a) investigate whether shear displacements could reduce the magnitude of GCL panel overlap during earthquake shaking; b) explore the influence of gravel particles on GCL thickness at localised point of contact; and c) observe the consequences of an accidental exposure of an uncovered GCL to short duration rainfall in terms of moisture content and effects during subsequent compaction.

The objectives of the study will be met through two separate full scale experiments. Firstly, the experiment of Sawada et al (2018) in which a 3 m high dam retrofitted with a continuous GCL (Figure 2a) will be replicated with two notable differences – the inclusion of a downslope lapped joint and the intentional placement of gravel particles at the surface of the GCL – foundation soil interface. Secondly, a compaction test plot will be conducted in which an uncovered GCL will be exposed to prescribed durations of rainfall and subsequent varying degrees of compaction of an overlying cover layer to observe the GCL properties upon exhumation of the lapped GCL core.

2. MATERIALS AND METHODS

2.1 Full scale shaking table test

The shaking table test was performed at the same 3D full-scale earthquake testing facility used in the baseline study of Sawada et al., (2018) to permit a direct comparison of the new experiment with the behaviour of a nominally identical dam retrofitted with a continuous GCL. This facility, hosted by the National Research Institute for Earth Science and Disaster Resilience in Japan, is known within the earthquake engineering community as E-Defense (Tabata et al, 2017). Currently the world's largest shaking table, the 15 m × 20 m dimensions of the testing platform provide a unique opportunity to investigate the seismic behavior of full scale earth dams within purpose built steel strong box model containers (inside dimensions: length = 12.59 m; height = 3.55 m; width = 2.50 m; weight = 105 t). Additional details on these containers can be found in Sawada et al. (2018).

The geometry of the baseline experiment of Sawada et al., (2018) is presented in Figure 2a. With a height of 3 m, and a crest width of 1.5 m, the base of the dam was designed to a length of 10.5 m following Japanese guidelines of 1:1.5 side slopes (Ministry of Agriculture, Forestry and Fisheries, 2015a). The earth dam material was placed into 1000 kg capacity bags and hoisted into the strong box using a crane. A miniature excavator was then used within the strong box to place the material, before each 0.23 m thickness lift was finished by hand using rakes and densified with a vibrating roller and plate compactor resulting in a 0.2 m lift thickness of compacted material. The miniature excavator was then used to cut five 600 mm wide benches into the upstream slope of the earth dam (Figure 3a) to provide an average inclination of the benches of 1:1.5. As shown in Figure 2a, a bench rise of 0.3 m to

the first bench, followed by a rise of 0.6 m for subsequent benches enabled the overall average inclination of the benched slope to be parallel to the cover soil. The GCL was then placed, the cover soil compacted in lifts from the bottom of the dam up to the crest, and the miniature excavator used for final shaping of the upstream face of the dam. The upstream reservoir was then filled to a depth of 2.5 m allowing for 0.5 m of freeboard, and a filter mat was placed at the distal end of the reservoir to minimize the amplitude of water waves induced by shaking and reflected off of the container boundary. Moreover, to prevent leakage along the side wall of the soil container, the cohesive soil used to create the embankment materials was directly placed with a width of 100 mm along the wall.

The new earth dam test geometry, illustrated in Figure 2b, is nominally identical to the earth dam retrofitted with the continuous GCL of Figure 2a with two notable exceptions. Firstly, a 350 mm width lapped joint was included on the third bench. With the lower elevation GCL placed first, and the upper elevation GCL placed second, the top surface of the upper GCL of the overlap is intended to be tension should the cover soil experience shear displacement at the GCL – cover soil boundary. To ensure adequate hydraulic performance of the overlap, supplemental granular bentonite was applied with a target dry mass per unit area application rate of 8.9 kg/m^2 within the central 250 mm of the 350 mm overlap width. The second difference in the present study is the intentional inclusion five approximately 30 to 50 mm diameter gravel particles at the top surface of the bench. As illustrated in Figure 2b, these

particles were intentionally located on the lower two benches to ensure that any result local indentations within the GCL are subjected to the worst-case hydraulic conditions possible at the scale of the experiment (i.e. highest possible total head). The initial location of the GCL above each of these gravel particles was marked using paint (Figure 3b) for subsequent identification of any indentation and shear displacement at the location of the particle during the exhumation of the GCL after test completion.

The instrumentation sensor configuration for the earth dam experiment was designed to enable a direct comparison of seismic behavior of the two earth dam experiments. Therefore, whenever possible, identical sensor locations were chosen for the present study as were used by Sawada et al. (2018). The primary sensors include accelerometers, pore water pressure transducers, and laser displacement sensors denoted as “A”, “P”, and “D” respectively in Figure 4. The second digit of the alphanumeric sensor label denotes whether the sensor data belongs to the baseline experiment (Test 1, Sawada et al., 2018) or Test 2 (the present study). Subsequent digits correspond to the sensor number, and in the case of the displacement sensors, prefaced by an additional identifier to denote positon on the upstream face, crest, or downstream face as “J”, “T”, and “K”, respectively.

The profile of x-direction (i.e. horizontal) acceleration within the earth dam was measured using a network of nearly forty accelerometers (ASW-5AM36, Rated Capacity ±49.03 m/s^2, Rated Output 0.5

mV/V or more, Frequency Response 0 to 100Hz, Kyowa Electronic Instruments Co., Ltd.) placed at 0.6 m vertical spacing (i.e. every three lifts). Additional accelerometers were placed to measure acceleration in the z-direction (i.e. vertically) at the crest and the upper side slopes, and in three axes at the crest and at two elevations along the centerline of the earth dam. In the present study, the measurement of acceleration in three axes has been prioritized along the crest, upstream and downstream faces of the earth dam in the refined accelerometer layout in Figure 4. In another modification, accelerometers A2-23 and A2-24 were fixed to the upper and lower lapped GCL, respectively. The objective of this change is to provide a means of identifying any relative motion along the interface during earthquake shaking as this would be represented as a phase lag in the readings of these two sensors.

The profile of static and excess pore water pressure throughout the earth dam was measured using up to twenty-five 20 mm diameter pore water pressure transducers (BPR-A-200KPS, Rated Capacity 200 kPa, Rated Output 1 mV/V or more, Kyowa Electronic Instruments Co., Ltd.), each fitted with a 10 micron pore size stainless steel filter element, and placed at a 0.6 m vertical spacing (i.e. every three lifts). One pore pressure transducer in each test (P1-09 and P2-09) was installed on the bed of the upstream reservoir to measure the upstream water level. The pore water pressure transducers P1-01 to P1-08 and P2-01 to P2-08 were installed in the middle of the 0.2 m thick bed layer to capture the total head profile through the dam.

The displacements of the upstream slope above the waterline, the crest, and the downstream face of the dam were measured using laser displacement sensors (LK-500, Measuring Range 250 to 750 mm, Resolution 0.05 mm, and IL-2000, Measuring Range 1000 to 3500 mm, Resolution 0.5 mm, KEYENCE Corporation). These sensors measure displacement along the line of sight of the laser, illustrated as the vectors shown in Figure 4.

Simple sine waves of 5Hz in the transverse direction of the embankment were used as input motion as the purpose of this study is to obtain benchmark data to compare to the results of numerical analyses, rather than to simulate earthquake damage of a specific dam to a specific event. The duration of shaking was 12 s, comprised of a 2 s duration ramp to the maximum acceleration, 8 s at the constant maximum acceleration value, followed by a 2 s ramp to zero acceleration. The choice of maximum acceleration magnitude was varied to investigate the performance of the earth dams to both Level-1 and Level-2 seismic motion, as described by the Japanese guideline (Ministry of Agriculture, Forestry and Fisheries, 2015b). Level 1 seismic motion consists of lower peak acceleration assumed to occur once or twice during the service life of the earth dam, whereas Level 2 shaking represents low probability, extremely strong seismic motion. For the sake of this paper, Level 1 shaking is taken to be a peak acceleration of approximately 170-180 Gal, and Level 2 shaking is greater than 470 Gal. The input accelerations tested

for the two earth dam models (Test 1, Test 2) are presented in Figure 5.

2.2 GCL hydration and compaction test plot

The objective of the second full-scale experiment is to investigate the consequences of low normal stress hydration of the GCL layer after varying degrees of compaction of an overlying cover soil layer. A 19.5 m long and 1.2 m wide test plot was conducted in which the same foundation soil used in the shaking table tests was levelled and compacted into a flat bed prior to placement of the GCL panel and compaction of two lifts of cover soil (Figure 6). Three experiments were then conducted: a) the virgin GCL was placed and covered in a timely fashion (i.e. hours) to investigate the case of hydration occurring only from the subsoil, b) the virgin GCL was placed on a tarp covering the foundation soil (i.e. to minimize gain or loss of water the foundation layer), sprayed with water, and allowed to experience low normal stress hydration for a period of 1.5 days prior to covering, and c) a control experiment was conducted in which the cover soil was simply placed and compacted in the absence of the GCL.

After the placement of each 0.23 m of cover soil, six 2 m long test sections of varying degrees of compaction was achieved through 0, 2, 4, 6, 8 10 passes of an approximately 800 kg vibrating roller (n.b. zero passes implies spreading of soil only). Nuclear density tests (NDT) and sand cone tests (SCT)

were then conducted within the compacted cover soil, the cover soil carefully removed to avoid damage to the GCL, and GCL samples (150 mm x 250 mm) collected in each section to measure the water content and the thickness of the GCL.

2.3 Materials

Soil

The soil used for both full scale tests (i.e. shaking table test and hydration test plot) was a cohesive soil containing particle sizes up to gravel size excavated from a borrow-pit in Hyogo prefecture, which was mixed with silica sand excavated from a borrow-pit in Kyoto prefecture to create a soil gradation representative of the non-select fill material historically used in old earth dams in Japan. This mixture, used in the previous full-shaking table tests (Sawada et al., 2018), was recreated in the present study and the success in reproducing the soil properties are illustrated in terms of particle size distribution (Figure 7a), compaction curves (Figure 7b), and shear modulus and the damping ratio (Figure 7c).

GCL

The GCL used in the present study is composed of granular bentonite sandwiched between a woven polypropylene cover geotextile and a nonwoven polypropylene carrier geotextile, which are needle-punched together. According to the product specifications, the thickness of the dry GCL exceeds 6 mm in its off-the-roll condition; the permeability coefficient is less than 5×10^{-11} m/s (ASTM D5887); and

the mass per unit area exceeds 4000 g/m^2 (4623 ±282 g/m^2). The unconfined hydration behavior of the GCL was explored by measuring the increase in GCL thickness and water content of GCL specimens submerged in water for up to 190 hours. These results, presented in Figure 8, indicate that the GCL achieves a steady-state moisture content and thickness after 48 h of hydration. This period of hydration was then adopted in the direct shear testing program to investigate the interface shear behavior of the GCL-soil interface.

The internal shear strength of GCLs and frictional properties of interfaces between GCLs and geomembranes (i.e. typical composite liner side slopes) have been examined by many researchers (e.g. Stark and Eid, 1996; Bargado et al., 2006; Vukelic et al., 2008). However, the interface friction relevant to the application of GCLs within earth dams is that of the GCL-soil interface, with comparatively less data published in the literature (e.g. Sasaki et al., 2015; Shigemoto et al., 2017; Suzuki et al., 2017). To place the subsequent observations of seismic performance of the earth dams during earthquake loading into the context of the shear properties of the interface, direct shear tests were performed between the embankment soil and the woven cover geotextile and the nonwoven carrier geotextile. These results were performed for effective confining stresses of 25, 50, and 100 kPa for GCLs in both the off-the-roll initially dry condition and after hydration under zero confining stress for 48 h. As expected from the literature, these results indicate that the hydrated specimens generally exhibited somewhat lower large

deformation shear strength values than that observed in its virgin dry condition (Figure 9c). Of particular importance, both the nonwoven and woven interface friction values were found to be nominally identical with interface friction angles of 32.5° and 37° for the hydrated and dry moisture conditions, respectively. If these values were to have differed, extra consideration would need to be placed on the orientation of the GCL during installation and the associated construction inspection to ensure the weaker of the two interfaces corresponds to assumptions made during the design of the structure.

3. RESULTS

3.1. Investigation of Possible Shear-Induced Reduction of Panel Overlap

The first objective of the present study is to investigate whether downslope displacements associated with Level 1 or Level 2 shaking could damage the barrier system through a shear-induced reduction of the length of GCL panel overlap. After subjecting each dam to Level-1 shaking, no apparent damage (e.g. cracks, excessive displacements, etc) were observed in either the continuous GCL or lapped GCL earth dam. Therefore, results are presented only for Level-2 shaking unless noted otherwise.

The accelerations measured at an elevation of 1.8 m of the 3 m tall earth dam are presented in Figure 10 for both the continuous GCL case (Test 1) and the lapped GCL case (Test2) for Level 2 shaking. As expected from the literature, accelerations at this elevation are significantly larger than the input base

acceleration due to amplification with height within the embankment, which is a typical dynamic characteristic of elastic bodies. At the upstream sides in both models, the measured accelerations are asymmetric. That is, the amplitude of acceleration in the positive direction is much larger than the negative direction. An explanation of this phenomena seen in Test 1 (Sawada et al., 2018) and reproduced herein in Test 2, is that the upstream face of the dam has a higher degree of saturation, whereas the lower degree of saturation downstream face benefits from its augmented strength and stiffness associated with this lower degree of saturation.

The first non-destructive indication whether any potential slip and loss of GCL overlap can be observed from accelerometers A2-23 and A2-24, which were fixed to the upper and lower lapped GCL, respectively. The time history of acceleration measured at these two locations are plotted in Figure 11 in which any relative motion between these GCL panels would be represented as a phase lag in the readings of these two sensors. The lack of any phase lag therefore indicates that no relative motion of the GCL should be expected at this location during subsequent exhumation to confirm this finding.

Despite the apparent lack of relative displacement at the location of GCL overlap, the earth dam experienced significant deformation. The most easily recognizable external manifestation of this deformation is the appearance of longitudinal cracks along the crest of the embankment dam in both

earth dam models (Figure 12). To track the vertical extent of these cracks, a dilute mixture of lime and water was poured into the cracks for subsequent identification during post-mortem examinations of the earth dams. Isometric view photographs of the top benches after the careful removal of the upstream face of each dam indicate that the crack extended through the 300 mm of cover soil on top of the GCL and approximately one-half to two-thirds of the height of the uppermost bench (Figure 13a, b) consistent with a hypothesized shear surface outside of the zone of benched soil (Figure 13c). Due to the non-transparent side walls of the strong box containers in which the experiments were performed, additional work would be required to confirm the location and shape of shear surface.

Additional excavation to the depth of the overlapped GCL joint in Test 2 enables a confirmation of the observation of no relative motion along the GCL overlap through physical measurements. Marker lines made at this location, highlighted with a dotted line in Figure 13b, confirm the findings that no change in overlap length occurred during Level 1 and Level 2 shaking. Whereas a single test cannot provide definitive evidence that shear displacements will never reduce the length of overlap at lapped joints in the downslope direction in every earth dam scenario, it does indicate that, for the conditions tested, this potential damage mechanism was not a relevant concern.

3.2. Gravel Indentation and Heightened Susceptibility to Internal Erosion

The second objective of the present study was to explore and quantify the degree of thinning of a GCL's bentonite core that can occur at points of localised contact with gravel particles often contained within the non-select backfill used in earth dam construction. This damage mechanism begins during compaction of the upstream face of the dam, and can be significantly exacerbated if shear displacement were to plow an elongated void in the GCL of reduced bentonite thickness. In both cases, the concern for the competency of the barrier system is that indentation by gravel particles have been shown to lower the total head required to initiate internal erosion through the bentonite core of the GCL.

The position of five gravel particles that were not removed from the surface of the lower two benches of the earth dam are identified in Figure 3 with an "x". At the completion of the measurements of GCL panel overlap, the remainder of the upstream face of the dam was carefully removed to expose the GCL at these locations and approximately 200 x 200 mm samples of the GCL were cut from the GCL panel. These samples were then turned over to expose the underside of the GCL, and the gravel particle protruding from the top surface of the embankment dam soil to illustrate the nature of the gravel indentation. These photographs, presented in Figure 14, illustrate that a significant amount of indentation has occurred and that the magnitude of the thickness reduction should be expected to vary considerably based on the geometry and size of the gravel particle protruding from the foundation soil. However, the shape of the indentation matches the shape of the gravel indentor, indicative of no

significant shear displacement having occurred between the underlying gravel particle and the GCL.

The gravel particle and the GCL samples were then removed from the earth dam and a cross-section containing the maximum reduction in thickness identified (Figure 15a). Once cut, this cross-section enabled a view of the bentonite microstructure and the spatial variation of the bentonite core (Figure 15b), which could be quantified using Vernier calipers (Figure 15c). The results of the thickness measurements at the five sampling locations are presented in Figure 16. Whereas the hydrated thickness of the GCL away from the gravel indentation ranged from 8.6 – 12 mm, the thinnest location under the gravel particle was observed to be 2.2 mm. The consequence of such a reduction in thickness of a GCL was investigated in the laboratory by Dickinson and Brachman (2010) in the context of gravel indentation in GCLs within landfill liner applications. This work illustrated that a gravel particle reducing the GCL thickness to 2 mm could reduce the total head difference across the GCL to initiate internal erosion to approximately 80 m in the case of no geotextile above the GCL, and to approximately 1 m if a geotextile was placed on top of the GCL. This difference was attributed by these authors to the interface transmissivity of the geotextile delivering fluid pressure to the point of weakness. In the context of earth dams, these laboratory findings indicate that no internal erosion should have been experienced due to the 2.2 m head above the GCL since the gravel particle remained imbedded in the GCL. However, if the gravel particle were to have plowed an elongated thin zone in the bentonite core

of the GCL, the risk of internal erosion through the GCL barrier cannot be ruled out.

To investigate whether any leakage occurred, the results of excess pore water pressure from the network of pore water pressure sensors located at the upstream and downstream sides of the GCL overlap and the location of the gravel inclusions are plotted during Level 2 shaking in Figure 17. In order to present both the short-term generation of excess pore water pressure during shaking and the long-term dissipation of water pressure, time presented on the x-axis of Figure 17 switches to a logarithmic scale after 20 s of shaking. During shaking, pore pressure sensors on the more highly saturated upstream side of the GCL (P2-15, 20, 23) experience negative excess pore water pressures whereas those on the more unsaturated downstream side of the GCL (P2-13, 18) experience slight positive pore water pressures. This behavior, also observed in Test 1 by Sawada et al., (2018) is hypothesized to be due to upstream side having sufficient degree of saturation to behave in undrained (i.e. no volume change) during the duration of shaking. After shaking, the long term monitoring of the pore pressure sensor (P2-09) indicates that the water surface elevation in the reservoir did not change, illustrating that no significant leakage occurred during this time.

3.3 Potential GCL Damage due to Low Normal Stress Hydration

The third and final objective was to observe the consequences of an accidental exposure of an uncovered

GCL to short duration rainfall in terms of moisture content and effects during subsequent compaction. The GCL used in the present study was installed, woven face up, on a foundation consisting of a compacted leveled foundation soil covered by a blue tarp. The intention of the tarp was to quantify the increase in moisture content of the GCL from rainfall in isolation from the natural uptake of moisture from the foundation subsoil. Wetting of the top surface of the GCL was undertaken from both natural and artificial rainfall sources. The GCL was installed in the evening and experienced a light drizzle over night. In the morning, a hose was used to carry out watering at four times (at 8:30am, 10:30am, 1:30pm and 4:30pm). This resulted in a total time of low normal stress hydration of 23 hours. The GCL was then covered with two 0.2 m cover soil layers of varying degrees of compaction, prior to nuclear density tests and subsequent exhumation of GCL specimens to observe GCL thickness and moisture content. The experiment was then repeated for the case of no watering.

The results of the nuclear density tests indicate that the water content of the cover soil was consistently between 12-14 percent for all of the experiments (Figure 18a), enabling a direct comparison of the degree of compaction achieved in each of the test plots. As expected, neither the presence of the GCL nor the initial degree of hydration of the GCL (i.e. with watering or without watering) affected the compaction results (Figure 18b). Exhumation of the GCL specimens revealed that the GCL moisture content increased from the original off-the-roll value of 26.0 % to an average of 40.5 % due to 7 and

half hours of hydration from the cover soil only (i.e. without watering). For the case of the GCL intentionally exposed to natural and artificial rainfall, the water content observed in the six sampling locations was an average of 73.3 %, higher than that observed in samples experiencing hydration from the subsoil alone, but significantly lower than the 300% observed after 48h of submerged hydration. The thicknesses of the GCL mirrored these increases from the original off-the-roll value minimum thickness of 6.4 mm to averages of 6.8 mm and 7.8 mm after hydration from the subsoil and from watering, respectively. The observed increase in hydration depends on the GCL structure and the unsaturated properties of both the subsoil and the GCL, for example, the needle punched fibers and the initial moisture content of the subsoil (e.g. Beddoe et al., 2011; Rayhani et al., 2011). However, these results provide some additional evidence that short duration wetting prior to the application of normal stress (i.e. cover soil) does not necessarily result in hydration similar to the worst case scenario of the submerged zero normal stress condition. Given that the level of confining stress on GCLs in small earth dam retrofit applications post-construction is typically on the order of less than 1 m of cover soil on the upstream face, the degree of pre-hydration observed due to short duration watering is less than the final hydrated state post-reservoir filling.

5 CONCLUSIONS

Full scale testing was conducted to explore three potential GCL damage mechanisms in earth dam

retrofit applications in seismically active areas; in particular, to a) investigate whether shear displacements could reduce the magnitude of GCL panel overlap during earthquake shaking; b) explore the influence of gravel particles on GCL thickness at localised point of contact; and c) observe the consequences of an accidental exposure of an uncovered GCL to short duration rainfall in terms of moisture content and effects during subsequent compaction.

Experimental observations from the full scale earth dam test confirmed that no change in GCL overlap length occurred due to shear displacements associated with Level 2 shaking. Whereas a single test cannot provide definitive evidence that shear displacements will never reduce the length of overlap at lapped joints in the downslope direction in every earth dam scenario, it does indicate that, for the conditions tested, this potential damage mechanism was not a relevant concern. It is important to note that the interface friction characteristics of the cover and carrier faces of the GCL used in the present study were identical. If these values were to have differed, extra consideration would need to be placed on the orientation of the GCL during installation and the associated construction inspection to ensure the weaker of the two interfaces corresponds to assumptions made during the design of the structure. In particular, if the weaker of the two interfaces were to be located on the bottom of the GCL, loss of GCL overlap may be an issue.

Five gravel particles were not removed from the top surface of the embankment dam soil prior to placement of the GCL panel to investigate the potential for damage due to gravel indentation. The results of the thickness measurements at the five sampling locations indicated that whereas the hydrated thickness of the GCL away from the gravel indentation ranged from 8.6 – 12 mm, the thinnest location under the gravel particle was observed to be 2.2 mm. However, the shape of the indentation in the GCL was observed to match the shape of the gravel indentor, indicative of no significant shear displacement having occurred between the underlying gravel particle and the GCL. Observations of the hydraulic head required to initiate internal erosion at gravel contacts by Dickinson and Brachman (2010) agree with the observation that no internal erosion was observed due to the 2.2 m head above the GCL since the gravel particle remained imbedded in the GCL. If the gravel particles were to have been placed on top of the GCL, it is possible that these particles could be more likely to have experienced shear deformation.

Finally, a test plot was conducted to observe the consequences of an accidental exposure of an uncovered GCL to short duration rainfall in terms of moisture content and effects during subsequent compaction. The results of this experiment indicate that the water content of the GCL at the six sampling locations was an average of 73.3 %, higher than that observed in samples experiencing hydration from the subsoil alone, but significantly lower than the 300% observed after 48h of submerged hydration.

These results provide some additional evidence that short duration wetting prior to the application of normal stress (i.e. cover soil) does not necessarily result in hydration similar to the worst case scenario of the submerged zero normal stress condition.

These results indicate that although each of the three GCL damage mechanisms cannot be ruled out to ever occur in practice, the performance of the GCL retrofitted earth dam tested was satisfactory under even severe Level 2 earthquake shaking, and serves as a promising retrofit strategy to improve the static and seismic resistance of these structures.

ACKNOWLEDGEMENTS

This work was part of a collaborative research project between Hyogo prefecture and the National Research Institute for Earth Science and Disaster Resilience and a cooperative research project between Hyogo prefecture and Kobe University. The committee for disaster mitigation using E-Defense (Director: Tsuneo Okada, Emeritus Professor of Tokyo University) provided helpful suggestions and encouragement. The authors are grateful to Mr. Rintaro Shigemoto for his cooperation on the soil tests. In addition, the GCLs used in this work was provided by Volclay Japan Co., Ltd.

REFERENCES

Anderson, R., Rayhani, M.T., Rowe, R.K., 2012. Laboratory investigation of GCL hydration from clayey sand subsoil. Geotextiles and Geomembranes 31, 31-38.

Aoyama, M., 2011. Rehabilitation of Irrigation ponds using Bentonite sheets. Water, Land and Environmental Engineering 79(8), 44-45. (in Japanese)

Beddoe, R.A., Take, W.A., Rowe, R.K., 2011. Water-retention behavior of geosynthetic clay liners. Journal of Geotechnical and Geoenvironmental Engineering 137(11), 1028-1038.

Bergado, D.T., Ramana, G.V., Sia, H.I., Varun., 2006. Evaluation of interface shear strength of composite liner system and stability analysis for a landfill lining system in Thailand. Geotextiles and Geomembranes 24(6), 371-393.

Dickinson, S., Brachman, R.W.I., 2010. Permeability and internal erosion of a GCL beneath coarse gravel. Geosynthetics International 17(3), 112–123.

Lake, C.B., Rowe, R.K., 2000. Swelling characteristics of needlepunched, thermally treated geosynthetic clay liners. Geotextiles and Geomembranes 18(2), 77-101.

Ministry of Agriculture, Forestry and Fisheries, 2018. Small earth dam: <http://www.maff.go.jp/j/nousin/bousai/bousai_saigai/b_tameike/>. (in Japanese)

Ministry of Agriculture, Forestry and Fisheries: Design guideline of land improvement project “Small earth dam,” 2015a. (in Japanese)

Ministry of Agriculture, Forestry and Fisheries: Design guideline of land improvement project “Seismic

design," 2015b. (in Japanese)

Nakazawa, H., Sawada, Y., Oda, T., Kobayashi, T., Kobayashi, S., Kawabata, T., Shibuya, S., Kataoka, S., Yamashita, T., 2017. Characteristics on residual deformation of small earth dams in full-scale shaking table tests. Journal of Japan Society of Civil Engineers, Ser. A1 (Structural Engineering & Earthquake Engineering. 73, I_815-I_826. (in Japanese)

Oda, T., Sawada, Y., Nakazawa, H., Kobayashi, S., T., Shibuya, S., Kawabata, T., 2016. Influence of geosynthetics clay liner laid in a staircase shape in embankment on seismic behavior of small earth dam. Geosynthetics Engineering Journal 31, 175-182. (in Japanese)

Petrov, R.J., Rowe, R.K., Quigley, R.M., 1997. Selected factors influencing GCL hydraulic conductivity. Journal of Geotechnical and Geoenvironmental Engineering 123(8), 683–695.

Rayhani, M.T., Rowe, R.K., Brachman, R.W.I., Take, W.A., Siemens, G., 2011. Factors affecting GCL hydration under isothermal conditions. Geotextiles and Geomembranes 29(6), 525-533.

Rowe, R.K., Rayhani, M.T., Take, W.A., Siemens, G., Brachman, R.W.I., 2011. GCL hydration under simulated daily thermal cycles. Geosynthetics International 18(4), 196-205.

Sarabian, T., Rayhani, M.T., Hydration of geosynthetic clay liners from clay subsoil under simulated field conditions. Waste Management 33(1), 67-73.

Sawada, Y., Nakazawa, H., Kataoka, S., Kobayashi, S., Oda, T., Kobayashi, T., Shibuya, S., Yamashita, T., Tani, K., Kajiwara, K., Kawabata, T., 2016. Full-scale shaking table tests for small earth dams

with sloping core zone and geosynthetic clay lines. Geosynthetics Engineering Journal 31, 167-174. (in Japanese)

Sawada, Y., Nakazawa, H., Oda, T., Kobayashi, S., Shibuya, S., Kawabata, T., 2018. Seismic Performance of small earth dams with sloping core zones and geosynthetic clay liners using full-scale shaking table tests. Soils and Foundations 59(3), 519-533.

Shigemoto, R., Sawada, Y., Shimizu, K., Nishimura, T., Kaminobu, K., Kawabata, T., 2017. Mechanical characteristics of geosynthetic clay liners installed in small earth dams. Proceedings of the 2017 Annual meeting of JSIDRE, 610-611. (in Japanese)

Siemens, G., Take, W.A., Rowe, R.K., Brachman, R.W.I., 2012. Numerical investigation of transient hydration of unsaturated geosynthetic clay liners. Geosynthetics International 19(3), 232-251.

Stark, T.D. and Eid, H.T., 2006. Shear behavior of reinforced geosynthetic clay liners. Geosynthetics International 3(6), 771-786.

Suzuki, M., Koyama, A., Kochi, Y, Urabe, T., 2017. Interface shear strength between geosynthetic clay liner and covering soil on the embankment of an irrigation pond and stability evaluation of its widened sections. Soils and Foundations 57(2), 301-314.

Tabata, K., Nakazawa, H., Kajiwara, K., 2017. E-defense improved performance and possible geotechnical model tests on liquefaction behaviors for saturation evaluation, 16th World Conference on Earthquake, Paper no. 1492.

Vukelic, A., Szavits-Nossan, A., Kvasnicka, P., 2008. The influence of bentonite extrusion on shear strength of GCL/geomembrane interface. Geotextiles and Geomembranes 26(1), 82-90.

FIGURE CAPTIONS

Figure 1. Retrofitting of upstream face of small earth dam with GCL barrier.

Figure 2. Full scale shaking table experiments contrasting seismic performance of3 m high earth dams retrofitted with a) a continuous GCL (modified from Sawada et al., 2016), and b) GCL barriers subject to possible damage at locations of overlapped joints and gravel particles at the GCL-foundation soil interface.

Figure 3. Construction photographs illustrating a) shaping of benches in foundation soil comprising the upstream slope of the earth dam using a mini-excavator, and b) initial placement of GCL layer highlighting locations of gravel inclusions.

Figure 4. a) Accelerometer, b) pore pressure, and displacement sensors locations for continuous GCL (Test 1; Sawada et al., 2018) and c), d) lapped GCL experiment (Test 2, present study)

Figure 5. Input acceleration for shaking table tests on earth dam with continuous GCL (Test 1, Sawada et al., 2018) and lapped GCL (Test 2, Present study)

Figure 6. Test plot to investigate the consequences of low normal stress hydration on the GCL layer after varying degrees of compaction of an overlying cover soil layer (N = number of passes of 800 kg vibratory roller)

Figure 7. Properties of earth dam fill a) grain size, b) compaction properties, and c) non-linear stiffness and damping ratio

Figure 8. Unconfined hydration of GCL illustrating increase in moisture content and thickness with time

Figure 9. Shear strength of GCL-Soil interface on a) woven cover GTX, b) non-woven carrier GTX, and resulting c) Mohr-Coloumb failure envolope in dry and hydrated state (2 days of unconfined hydration)

Figure 10. Accelerations measured during Level 2 shaking for earth dam with continuous GCL (Test 1, Sawada et al., 2018) and lapped GCL (Test 2, Present study)

Figure 11. Acceleration measured on each side of the GCL panels comprising the overlapped joint in Test 2 during Level 2 shaking. Lack of evidence of phase difference is indicative of no relative motion and therefore no reduction of overlap at the joint

Figure 12. Surface expression of cracking in a) Test 1 (Sawada et al., 2018) and b) Test 2 (Present study).

Figure 13. Vertical extent of crack in dam crest inferred by inflow of dilute line-water mixture in a) Test 1 (Sawada et al., 2018), b) Test 2 (Present study), and c) hypothesised failure surface.

Figure 14. GCL samples of approximate dimensions of 200 x 200 mm, flipped to view underside of GCL to illustrate shape of gravel indentation and lack of evidence of relative motion between GCL and underlying gravel particle.

Figure 15. a) Selection of cross-section containing minimum GCL thickness, b) cut section, and c) measurement of minimum thickness

Figure 16. Reduction of thickness of GCL at each of the five gravel locations in the earth dam

Figure 17. Excess pore water pressure measured in Test 2 during Level 2 shaking. Lack of evidence of long term changes in pore pressure on downstream side of GCL indicative of no change to static water levels

Figure 18. Results of GCL hydration test plot experiment, a) consistency of moisture content of cover soil, b) variation in compaction of cover soil with compaction energy, c) GCL moisture content, and d) GCL thickness

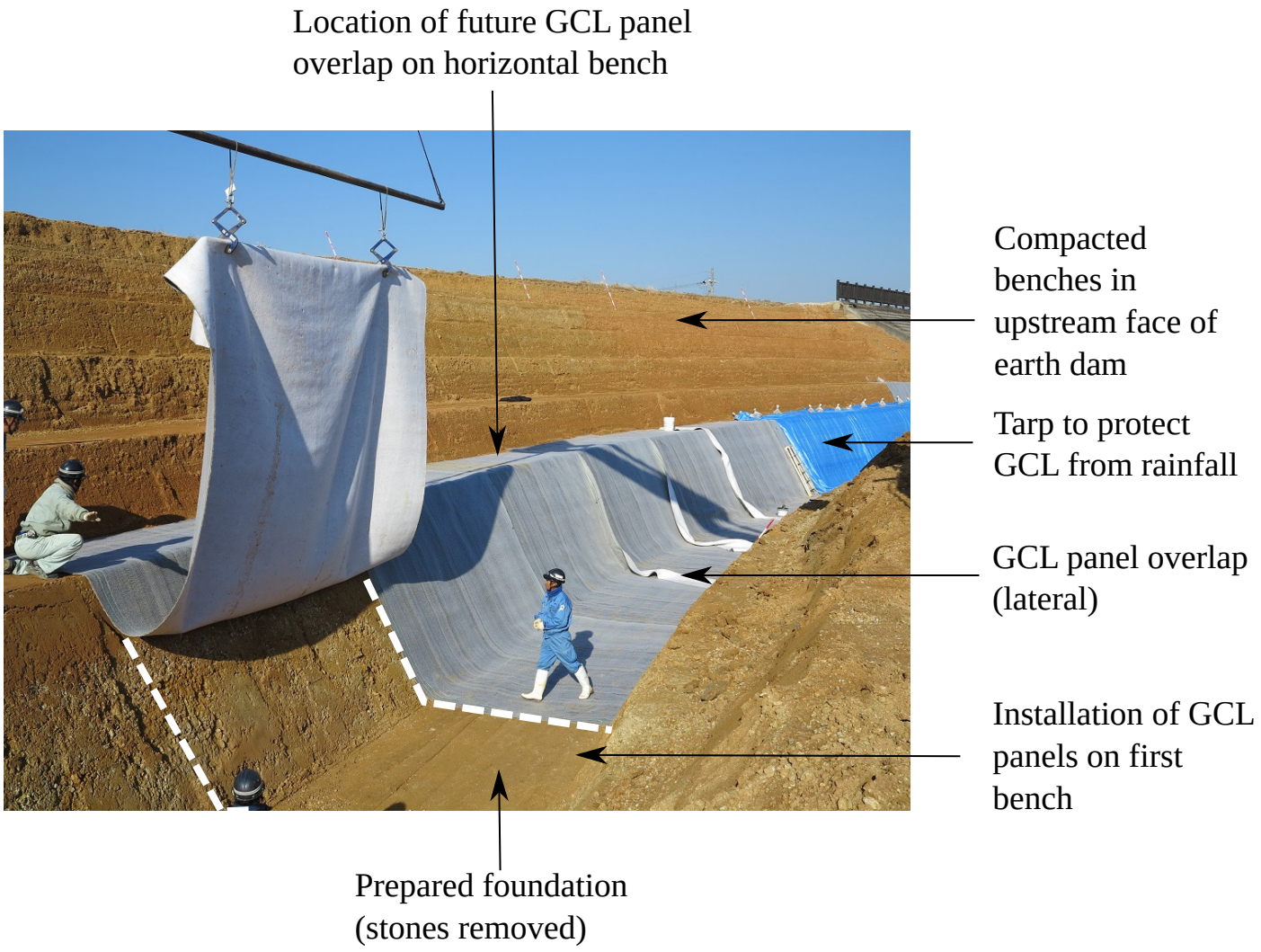

Figure 1. Retrofitting of upstream face of small earth dam with GCL barrier.

a)

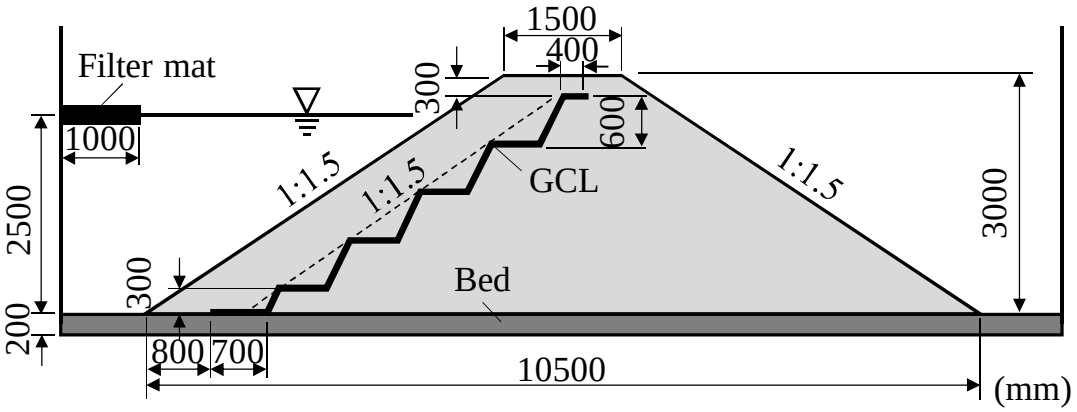

b)

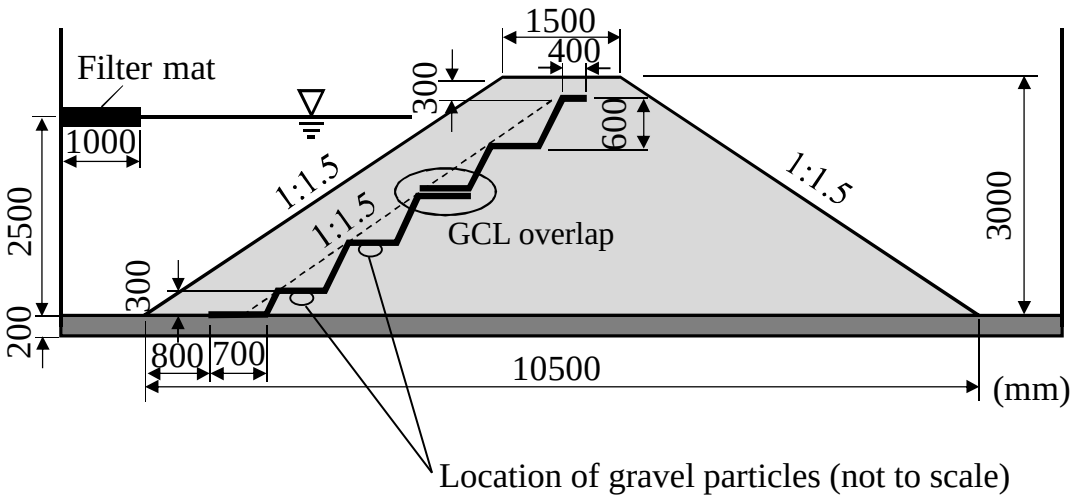

Figure 2. Full scale shaking table experiments contrasting seismic performance of 3 m high earth dams retrofitted with a) a continuous GCL (modified from Sawada et al., 2016), and b) GCL barriers subject to possible damage at locations of overlapped joints and gravel particles at the GCL-foundation soil interface

a)

b)

Figure 3. Construction photographs illustrating a) shaping of benches in foundation soil comprising the upstream slope of the earth dam using a mini-excavator, and b) initial placement of GCL layer highlighting locations of gravel inclusions.

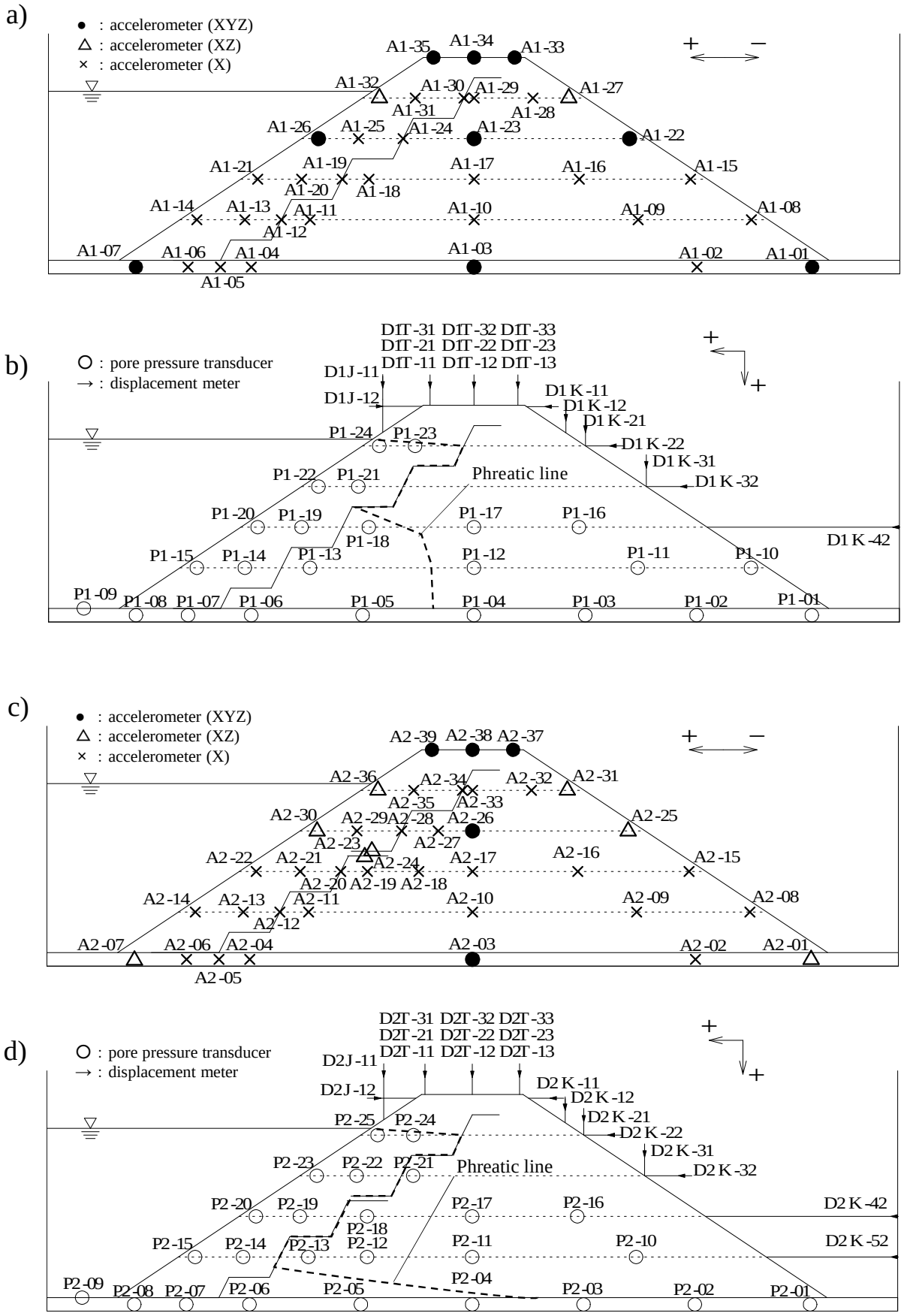

Figure 4. a) Accelerometer, b) pore pressure, and displacement sensors locations for continuous GCL (Test 1; Sawada et al., 2018) and c),d) lapped GCL experiment (Test 2, present study)

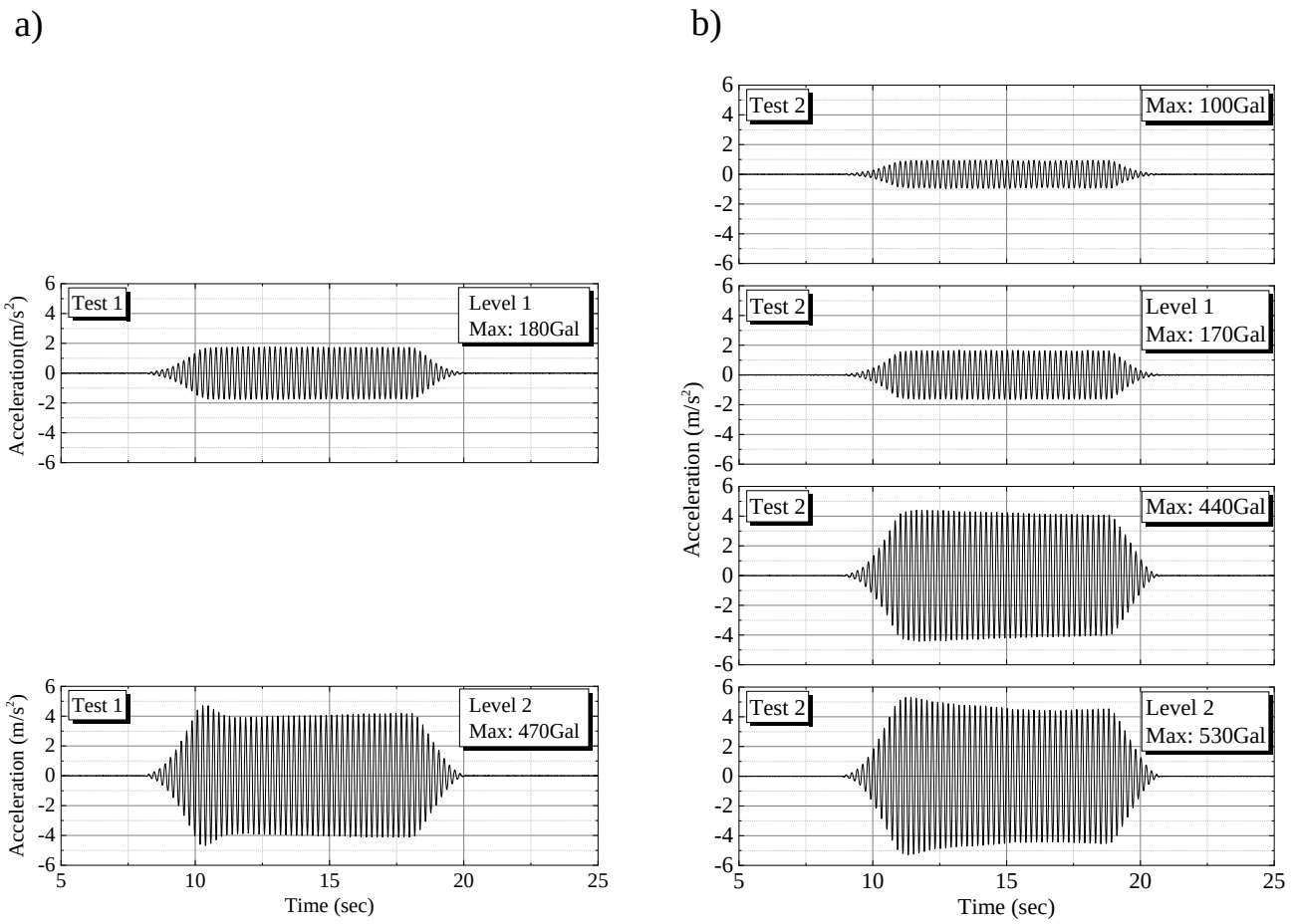

Figure 5. Input acceleration for shaking table tests on earth dam with continuous GCL (Test 1, Sawada et al., 2018) and lapped GCL (Test 2, Present study)

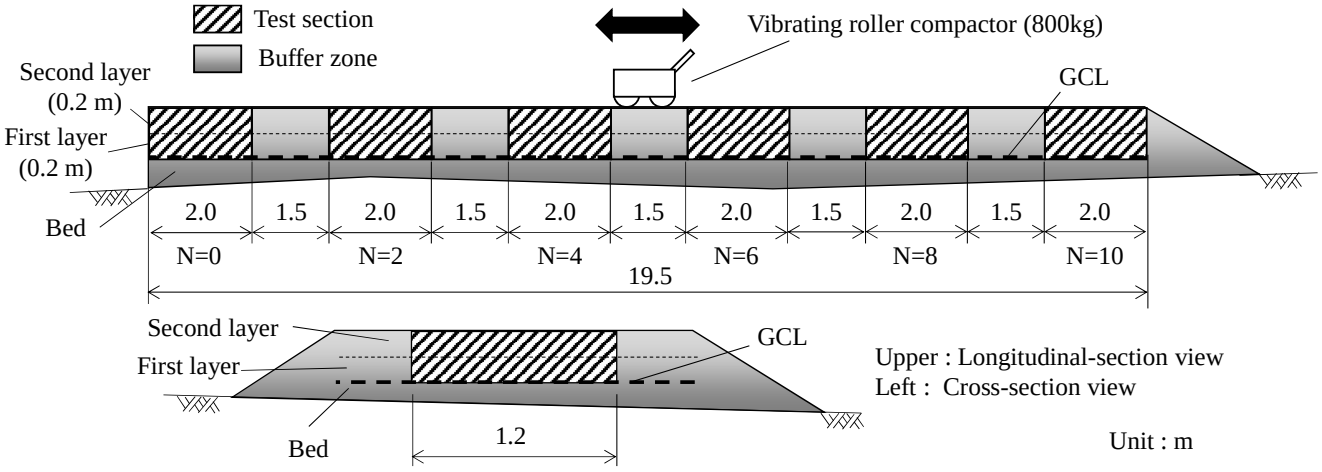

Figure 6. Test plot to investigate the consequences of low normal stress hydration on the GCL layer after varying degrees of compaction of an overlying cover soil layer (N = number of passes of 800 kg vibratory roller)

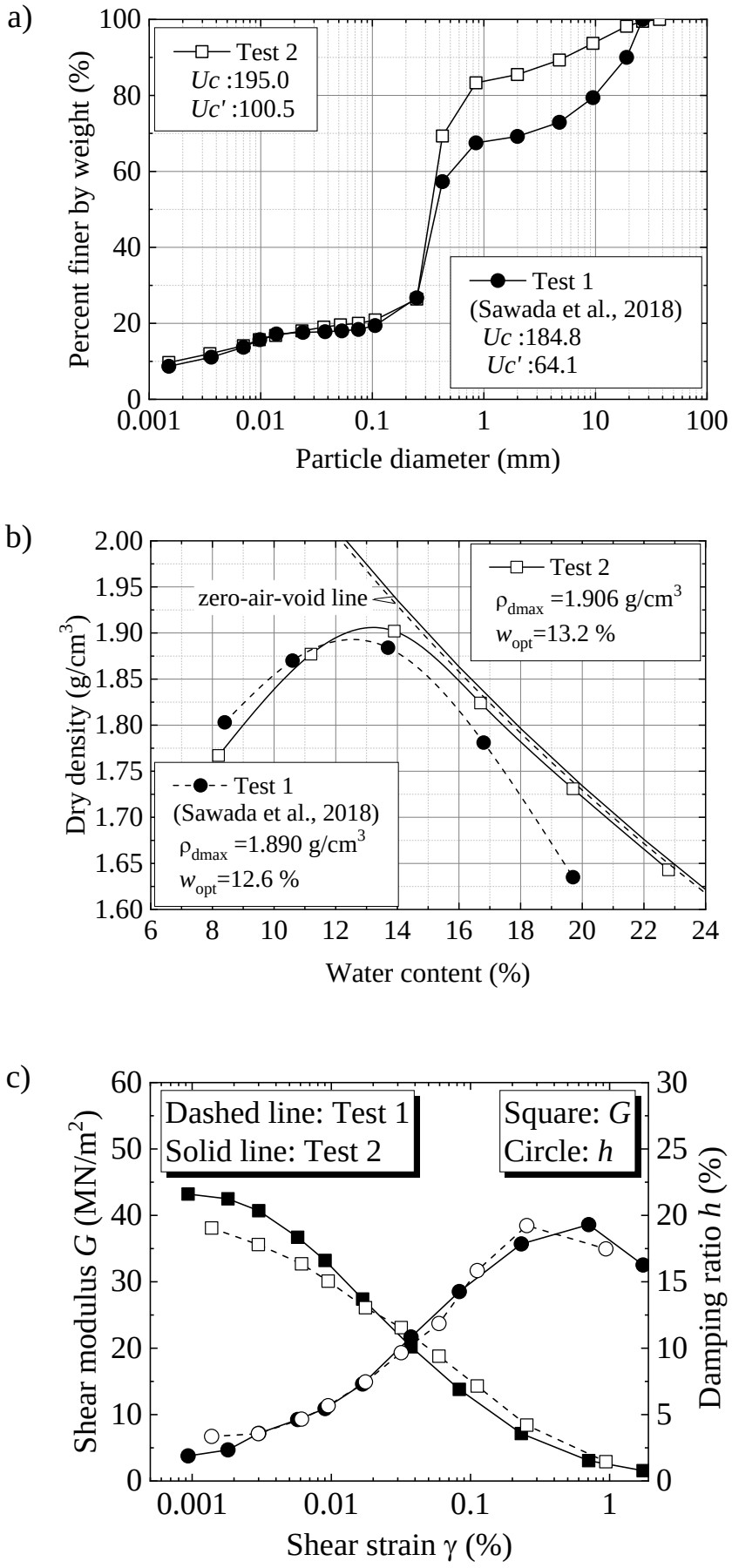

Figure 7. Properties of earth dam fill a) grain size, b) compaction properties, and c) non-linear stiffness and damping ratio

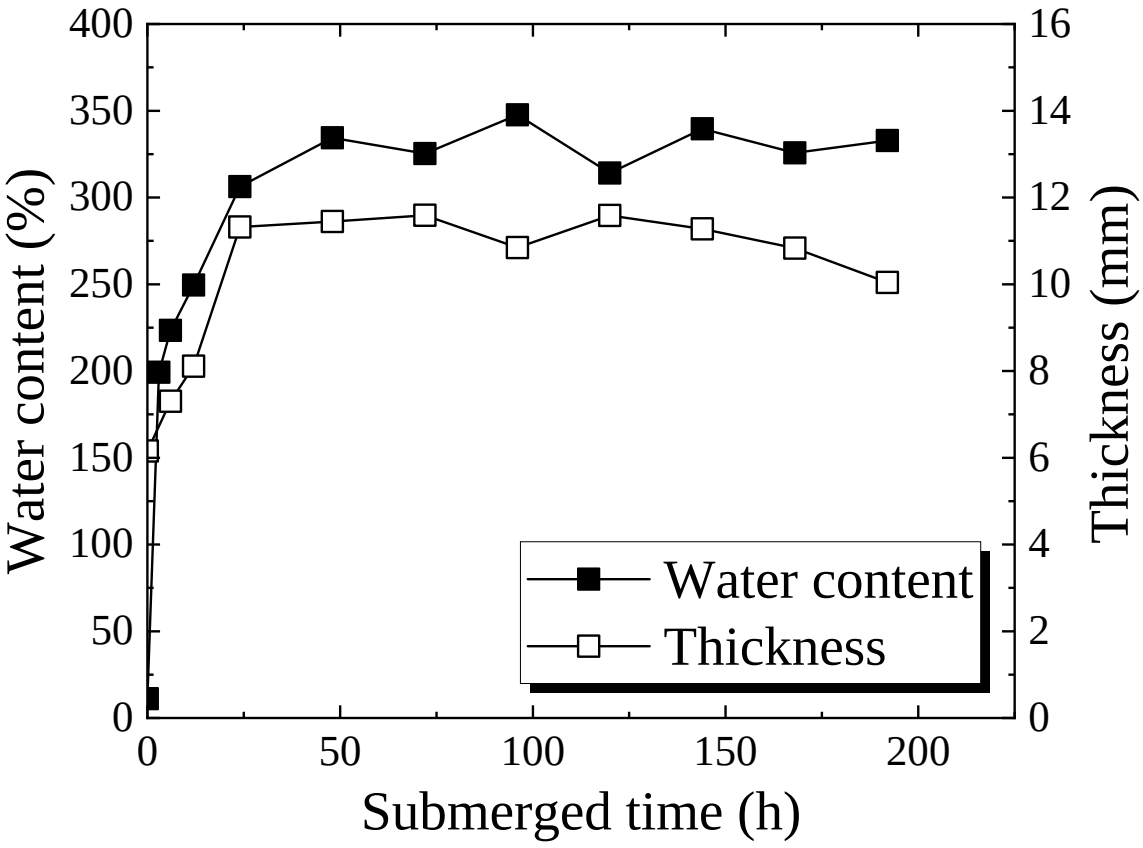

Figure 8. Unconfined hydration of GCL illustrating increase in moisture content and thickness with time

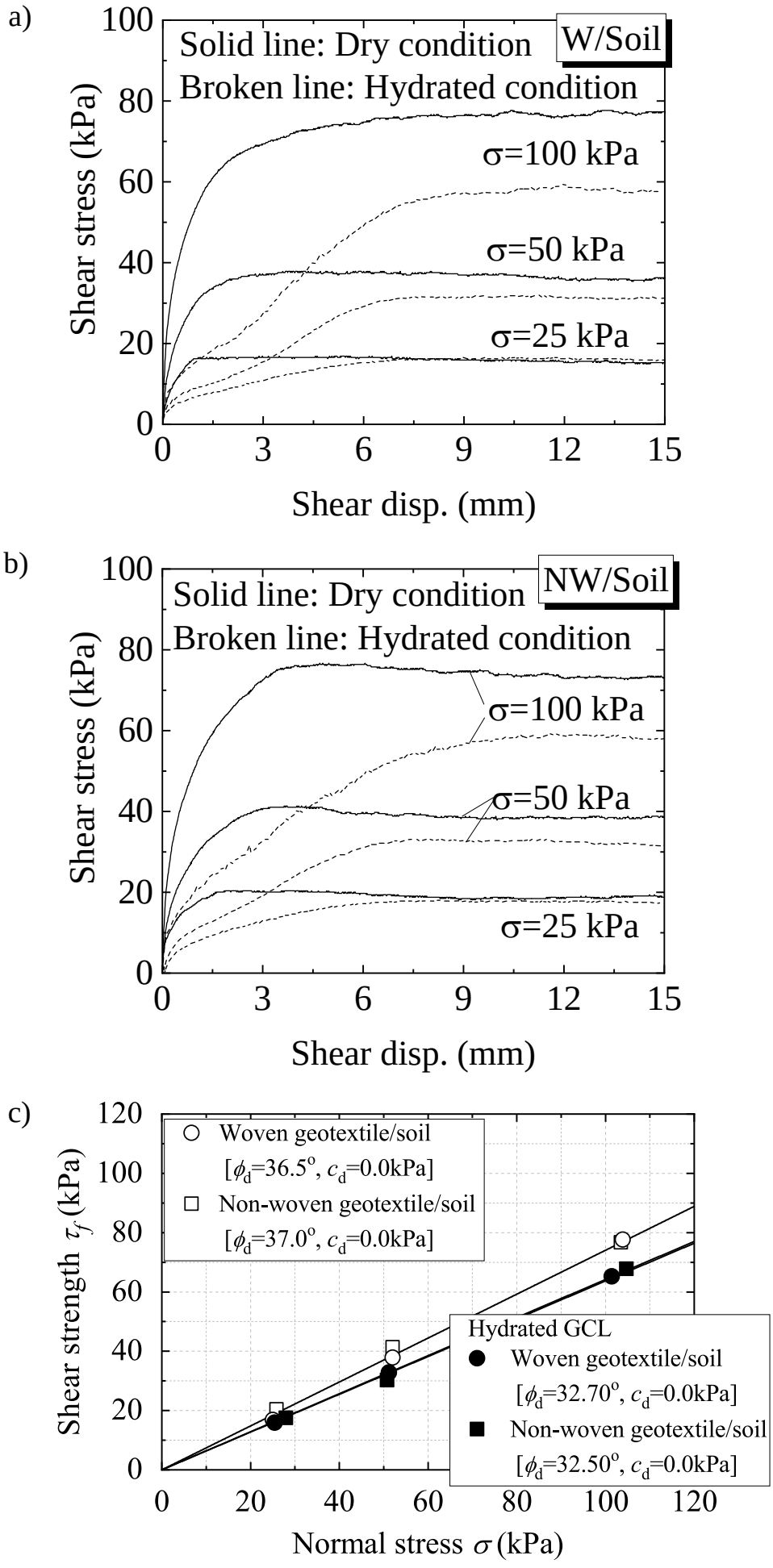

Figure 9. Shear strength of GCL-Soil interface on a) woven cover GTX, b) non-woven carrier GTX, and resulting c) Mohr-Coloumb failure envelope in dry and hydrated state (2 days of unconfined hydration)

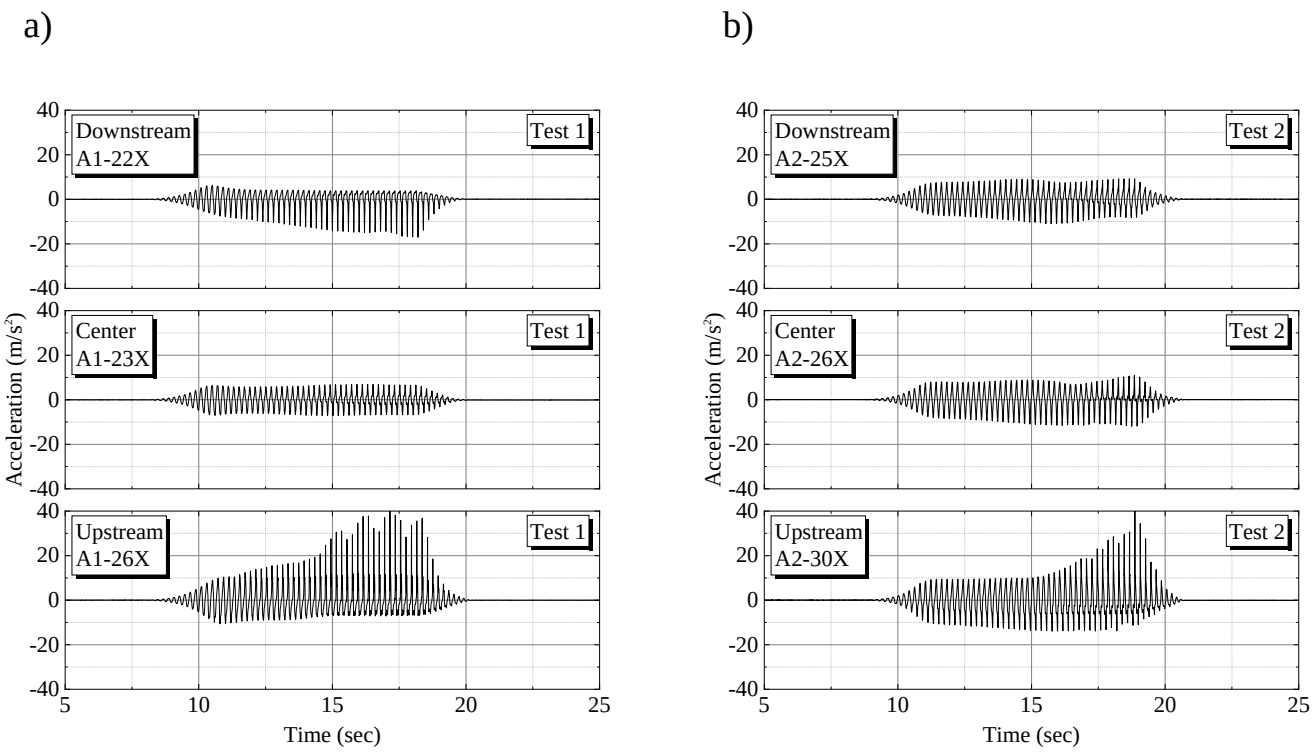

Figure 10. Accelerations measured during Level 2 shaking for earth dam with continuous GCL (Test 1, Sawada et al., 2018) and lapped GCL (Test 2, Present study)

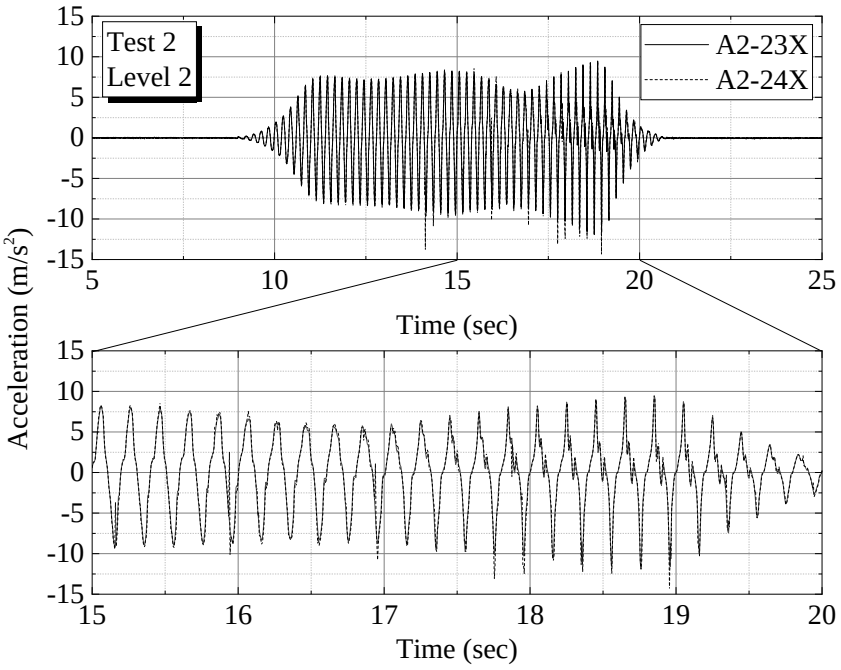

Figure 11. Acceleration measured on each side of the GCL panels comprising the overlapped joint in Test 2 during Level 2 shaking. Lack of evidence of phase difference is indicative of no relative motion and therefore no reduction of overlap at the joint

a)

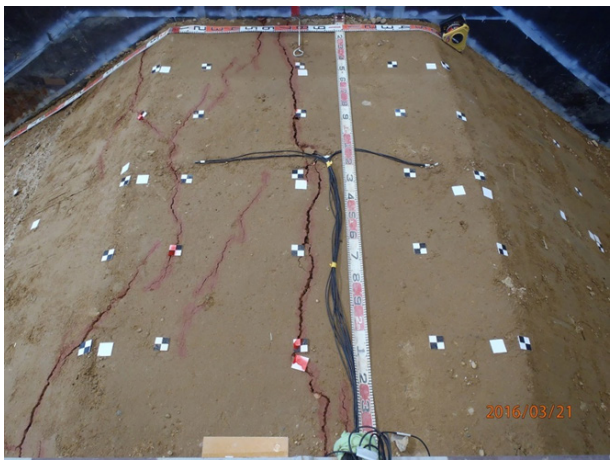

b)

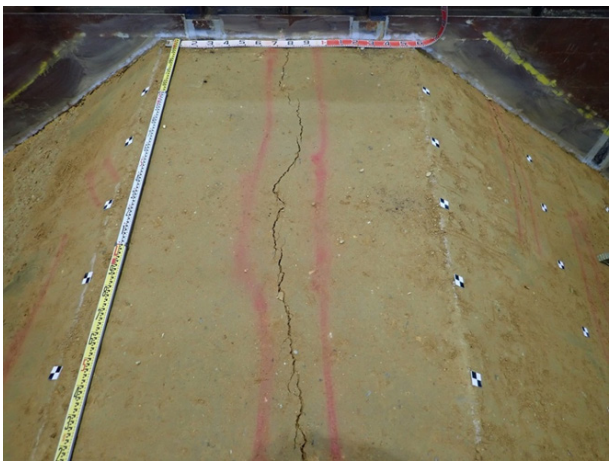

Figure 12. Surface expression of cracking in a) Test 1 (Sawada et al., 2018) and b) Test 2 (Present study).

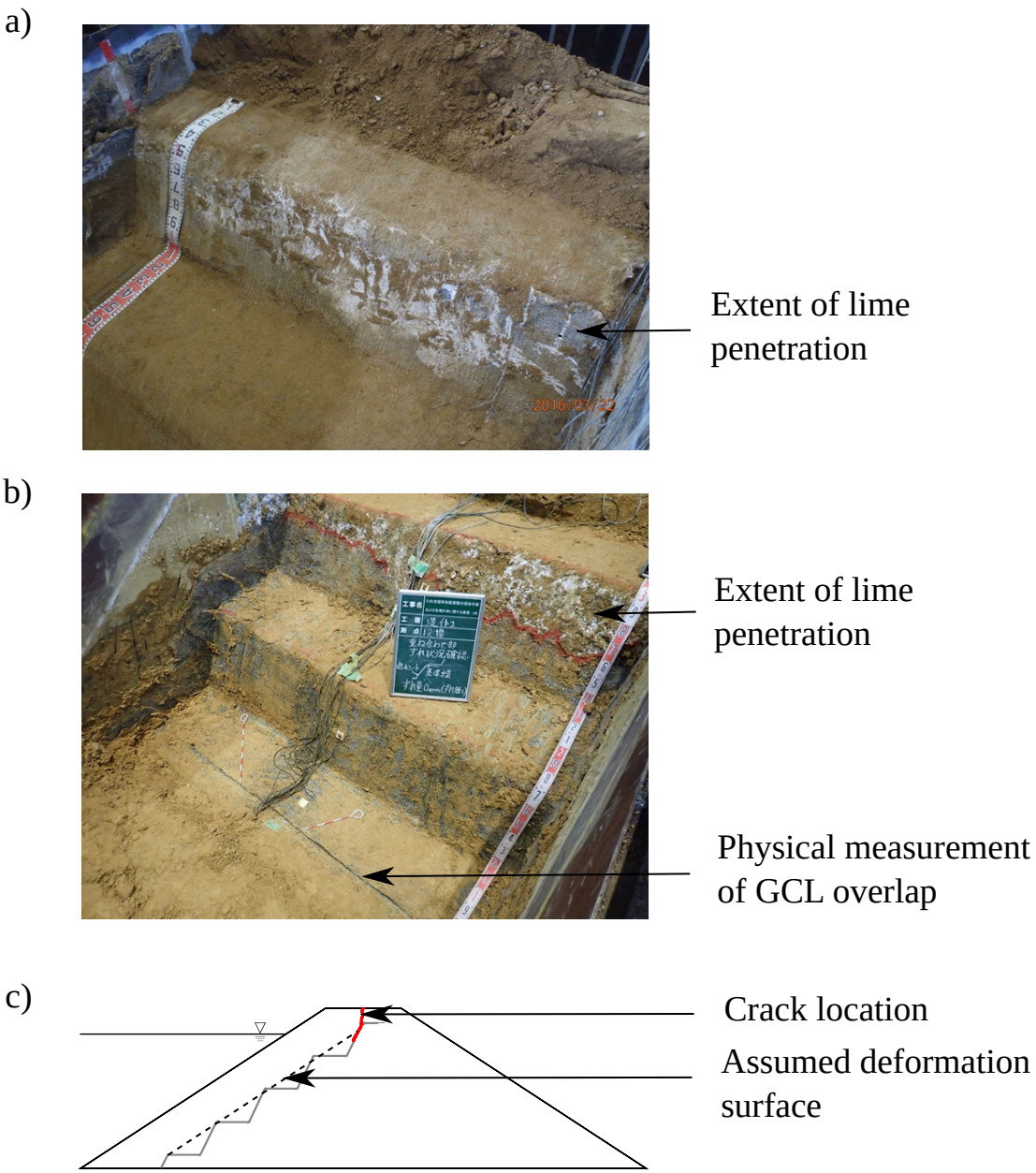

Figure 13. Vertical extent of crack in dam crest inferred by inflow of dilute line-water mixture in a) Test 1 (Sawada et al., 2018), b) Test 2 (Present study), and c) hypothesised failure surface.

a)

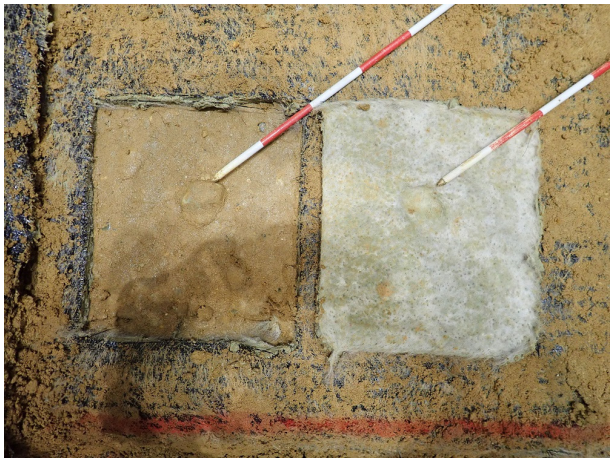

b)

Figure 14. GCL samples of approximate dimensions of 200 x 200 mm, flipped to view underside of GCL to illustrate shape of gravel indentation and lack of evidence of relative motion between GCL and underlying gravel particle.

a)

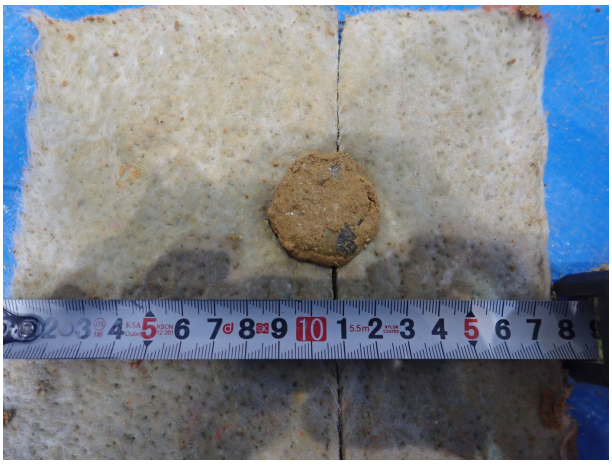

b)

c)

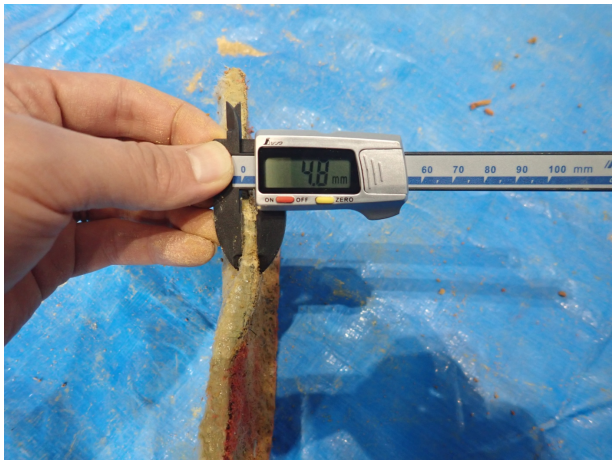

Figure 15. a) Selection of cross-section containing minimum GCL thickness, b) cut section, and c) measurement of minimum thickness

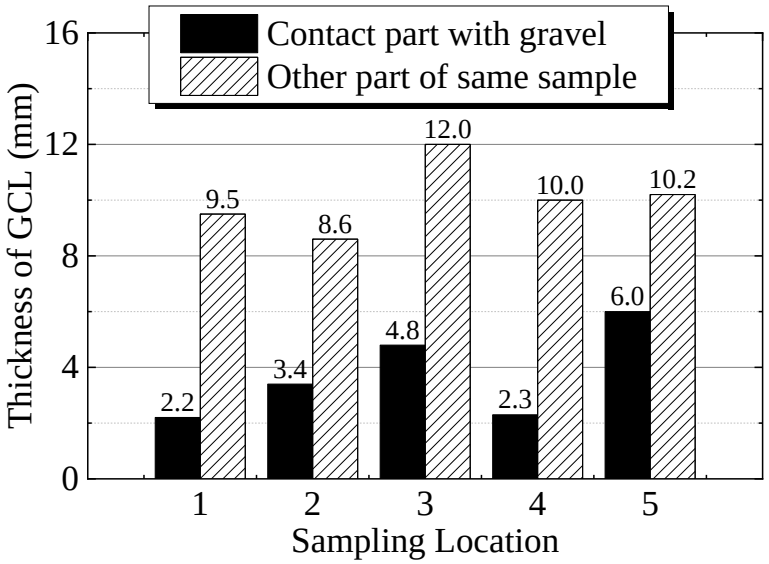

Figure 16. Reduction of thickness of GCL at each of the five gravel locations in the earth dam

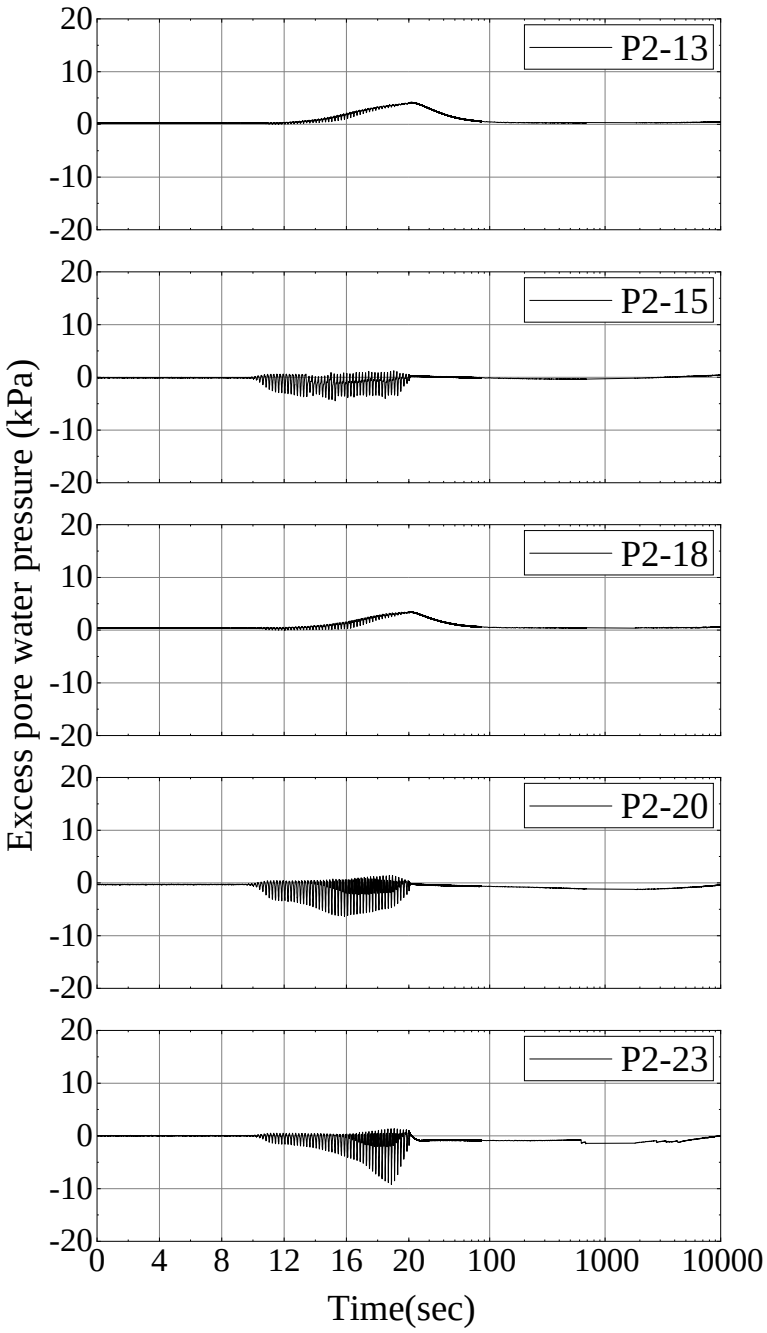

Figure 17. Excess pore water pressure measured in Test 2 during Level 2 shaking. Lack of evidence of long term changes in pore pressure on downstream side of GCL indicative of no change to static water levels

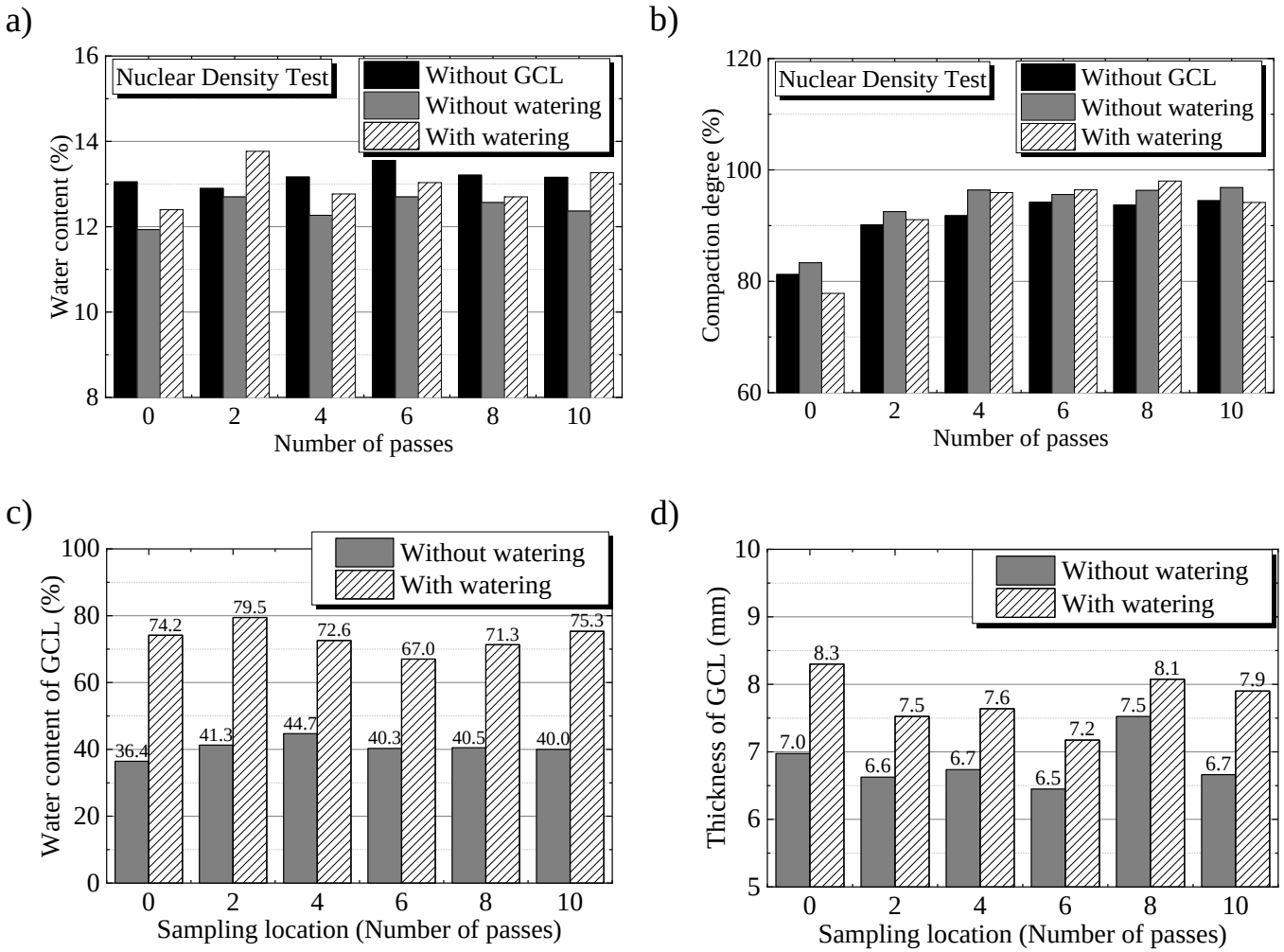

Figure 18. Results of GCL hydration test plot experiment, a) consistency of moisture content of cover soil, b) variation in compaction of cover soil with compaction energy, c) GCL moisture content, and d) GCL thickness